FORMATION MECHANISM OF PLATE-LIKE ICE CRYSTALS GROWING IN AIR AT LOW TEMPERATURE AND LOW SUPERSATURATION

Takehiko Gonda[1], Yuki Matsuura[2] and Makoto Wada[3]

[1]*Division of General Education, Aichi Gakuin University, Araike, Iwasaki-cho, Nisshin 470-01*
[2]*Research and Development Center, Toshiba Corporation, Komukai, Toshiba-cho, Saiwai-ku, Kawasaki 210*
[3]*National Institute of Polar Research, 9–10, Kaga 1-chome, Itabashi-ku, Tokyo 173*

Abstract: The supersaturation dependences on the slope of growth hillocks formed on the $\{10\bar{1}0\}$ face P_P and the $\{0001\}$ face P_B of ice crystals grown in air at $-28.5°C$ and low supersaturation were measured to study the formation mechanism of plate-like ice crystals growing under this condition. As a result, it was found that both the $\{10\bar{1}0\}$ and $\{0001\}$ faces of plate-like ice crystals grown at $-28.5°C$ and low supersaturation grew by the Burton-Cabrera-Frank (BCF) mechanism, and when the relationship $P_P > P_B$ held, plate-like ice crystals grew.

1. Introduction

It is known that single columnar ice crystals grow below $-20°C$ (Nakaya, 1954; Kobayashi, 1961). Kikuchi and Hogan (1979) have observed diamond dust particles at South Pole Station at temperatures from -35 to $-37°C$ and have found plate-like ice crystals in the particles. Kuroda and Lacmann (1982) theoretically investigated the mechanism of the habit change of snow crystals with temperature and pointed out the possibility that plate-like ice crystals grew below $-20°C$ and at low supersaturation. Gonda and Koike (1982) experimentally found that plate-like ice crystals grew at -30 and $-35°C$ and at low supersaturation when the crystal size was small. This is applicable to minute ice crystals growing below $-40°C$ (Gonda, 1983). Gonda *et al.* (1986) qualitatively discussed the formation mechanism of plate-like ice crystals growing at low temperature and low supersaturation. In this paper, the surface patterns on plate-like ice crystals were observed by using a differential interference microscope and laser two-beam interferometry, and the formation mechanism of plate-like ice crystals growing at low temperature and low supersaturation is discussed.

2. Experimental Procedures

A schematic diagram of an experimental apparatus was described in a previous paper (Gonda *et al.*, 1994). In this paper, the construction of a growth chamber and the experimental method are briefly described.

Figure 1 shows the growth chamber used in this experiment. The central part of the chamber is composed of upper (T) and lower (U) copper plates. Their temperature is controlled independently by inserting thermal insulator (V) between them. In order to prevent inflow of heat into the growth chamber, it is covered by a thermal insulator. A
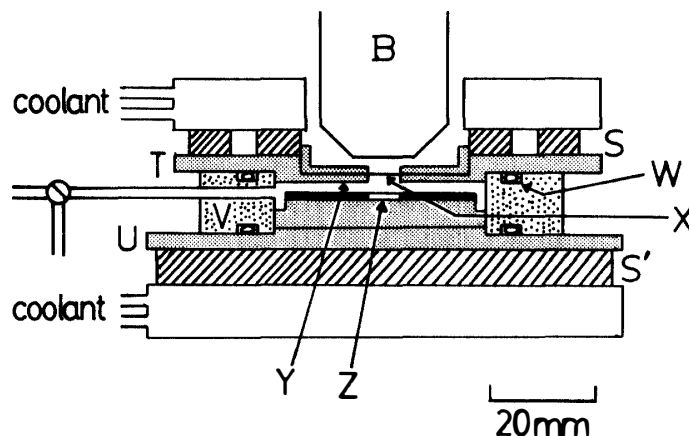
Fig. 1. Growth chamber for in situ observation of vapor-grown ice crystals. B: objective lens, S: thermoelectric module, S': thermoelectric panel, T: upper copper plate, U: lower copper plate, V: thermal insulator, W: O-ring, X:glass window, Y: water vapor supplier (high porosity metal), Z: glass substrate.

glass window (X) and an ice plate (Y) for water vapor source are attached on the inside wall of the upper plate. A glass window 0.2 mm thick is coated with a non-reflection film in order to remove light which is reflected by the glass window. An ice crystal is grown on a glass cover (Z) 0.2 mm thick and 6 mm in diameter whose under surface is blackened, which is attached to the lower plate. The lower plate is wholly covered by a teflon sheet in order to avoid nucleation of ice on it.

The experimental method is as follows. The growth chamber was cooled by circulating isopropyl alcohol. In order to control precisely the temperature of the upper (T) and lower (U) copper plates, the electric current which flows to the thermoelectric modules (S and S') was automatically controlled. The substrate temperature and the temperature difference between the upper and lower plates were measured using copper-constantan thermocouples. The measured values were automatically recorded in a microcomputer. In order to determine supersaturation precisely, the temperature difference between the upper and lower plates was held within $\pm 0.01\,°C$.

After the growth chamber was cooled to the specified temperature, a small amount of sufficiently diluted silver iodide smoke was inserted into the chamber. An ice crystal which was nucleated in air at low pressure was grown on the glass substrate. To grow the ice crystal under conditions which can ignore the volume diffusion process of water molecules and Berg effect, the air pressure in the chamber was held at 5.3×10 Pa. The growing ice crystal was observed *in situ* using laser two-beam interferometry. The differential interference images and interference fringes of equal thickness on the ice crystal surface were recorded by video tape recorders. Whenever each experiment was carried out, the temperature difference at which the ice crystal neither grows nor evaporates at a measured temperature was checked in order to determine supersaturation precisely.

3.   Analytical Equations

The slope of a growth hillock P on an ice crystal surface is obtained by the following equations.

3.1.   Method using interference fringes of equal thickness (Verma, 1953)
The slope of a growth hillock P is

$$P = \frac{\lambda \sin\theta}{2X},$$

where λ is the wave length of a laser beam, X the spacing of two adjacent interference fringes and 2θ the angle between interference fringes which bend at the top of a growth hillock.

3.2.   Method using Moiré fringes
The slope of a growth hillock P is

$$P = \frac{\lambda}{2L},$$

where L is the spacing between two adjacent Moiré fringes.

4.   Results and Discussion

The surface pattern of growing ice crystals was observed in situ using a differential interference microscope and laser two-beam interferometry.

Figure 2 shows the surface patterns on the (0001) face of an ice crystal grown in air of 5.3×10 Pa at −28.5°C and 5.0% supersaturation. Figure 2a is a differential interference image. Although a growth hillock is formed at the place indicated by an arrow, it is unclear in photograph. However, it can be detected by using laser two-beam interferometry. Figure 2b shows the interference fringes of equal thickness on the same crystal surface shown in Fig. 2a using two-beam interferometry. It is seen that the interference fringes bend at the top of the growth hillock. Here, we calculate the slope of the growth hillock to be 2.26×10^{-3}.

Figure 3 shows the surface patterns on the $(10\bar{1}0)$ face of an ice crystal grown in air of 5.3×10 Pa at −28.5°C and 2.3% supersaturation. Figure 3a shows the interference fringes of equal thickness on the $(10\bar{1}0)$ face. Although the interference fringes bend very slightly at the lower edge, we can hardly confirm them. In this case, we adopted the Moiré method in order to detect the slope of the growth hillock. Figure 3b is the Moiré patterns made by superimposing Fig. 3a and the interference fringes on the surface whose ice crystal is in a state of ice saturation. It is seen that semi-circular Moiré patterns are successively produced from the place indicated by an arrow. As the spacing between two adjacent Moiré patterns is 149.1 μm, the slope of the growth hillock is 2.12×10^{-3}.

Figure 4 shows the slope of growth hillocks measured on the $\{10\bar{1}0\}$ and $\{0001\}$
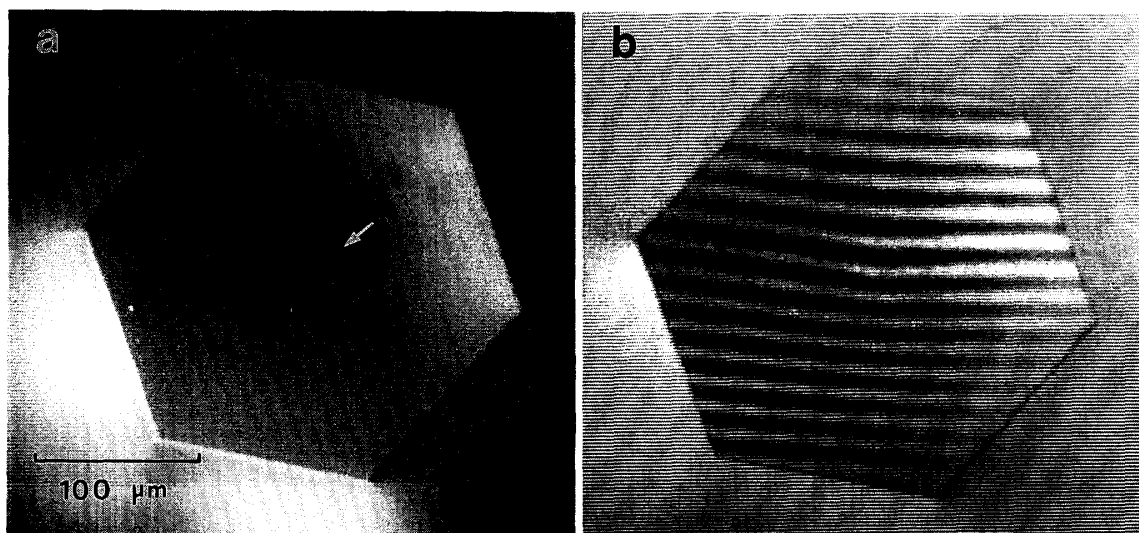
Fig. 2.   Surface patterns on the (0001) face of an ice crystal grown in air of 5.3×10 Pa at −28.5°C and 5.0%
supersaturation. (a) Differential interference image, (b) Interference fringes of equal thickness on
the same crystal surface as (a).
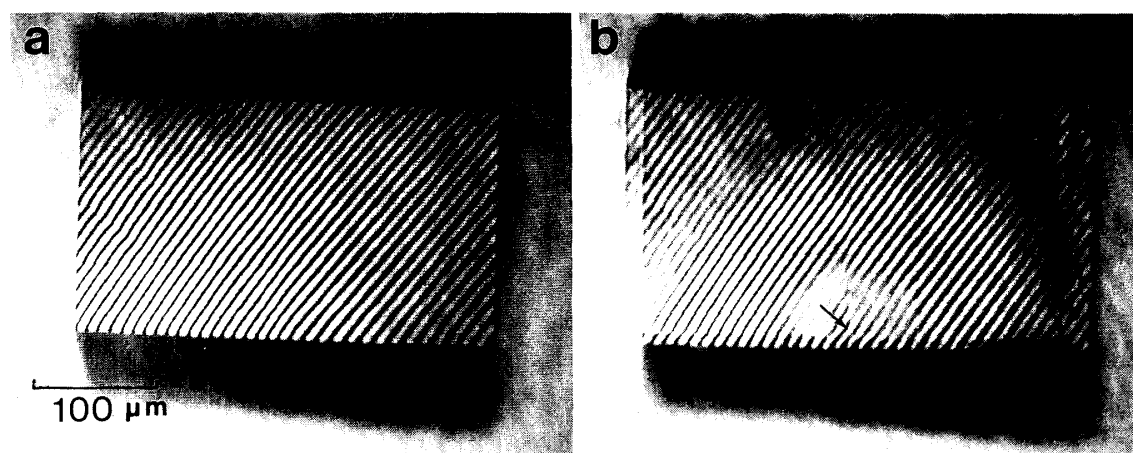
Fig. 3.   Surface patterns on the (10$\bar{1}$0) face of an ice crystal grown in air of 5.3×10 Pa at −28.5°C and 2.3%
supersaturation. (a) Interference fringes of equal thickness. (b) Moiré patterns on the same crystal
surface as (a).

faces of ice crystals grown in air of 5.3×10 Pa at −28.5°C *versus* supersaturation. The
solid and dotted lines in the figure are those drawn using the least square approximation.
The slope of the growth hillocks is proportional to supersaturation within the measured
range of supersaturation. Accordingly, it is known that ice crystals grown at −28.5°C and
low supersaturation grow by the Burton-Cabrera-Frank (BCF) mechanism. Here, the
slope of growth hillocks on the {10$\bar{1}$0} face was measured on ice crystals whose pris-
matic face grew parallel to the glass substrate, while that on the {0001} face was mea-
sured on ice crystals whose basal face grew parallel to the glass substrate. In the figure,
open circles are values on the {10$\bar{1}$0} face, while solid triangles and solid circles are
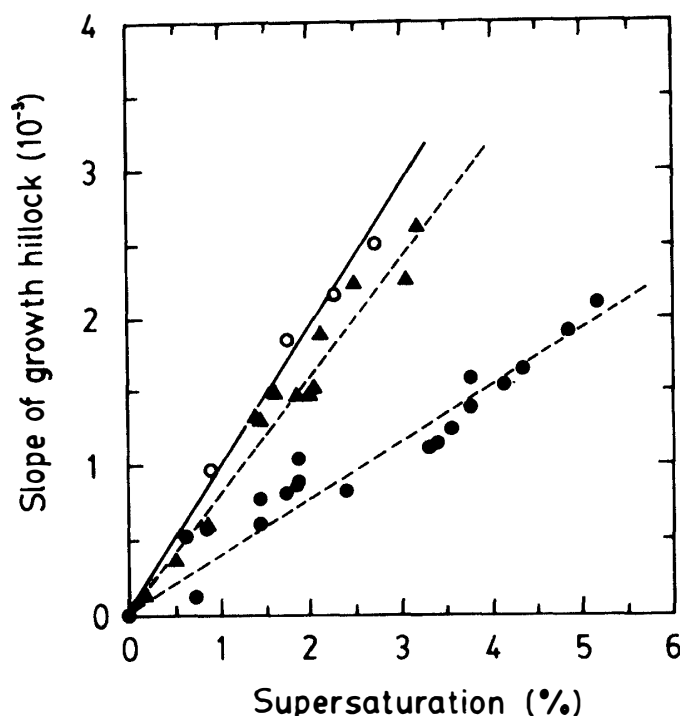
Fig. 4.   Slope of growth hillocks measured on ice crystals grown in air of 5.3×10
Pa at −28.5°C versus supersaturation. Open circles show the values on
the {10$\bar{1}$0} face. Solid triangles and solid circles show the values on
the {0001} face.

values on the {0001} face. Accordingly, there are two types of growth hillocks on the {0001} face. This means that two kinds of dislocations may outcrop on the {0001} face of ice crystals growing at −28.5°C.

Maiwa *et al.* (1990) have found that two kinds of dislocations outcrop on the (111) face of Ba $(NO_3)_2$ crystals and the slope of a growth hillock due to a screw dislocation is steeper than that due to a mixed dislocation. Moreover, they have found that when two kinds of dislocations outcrop on the (111) face at the same time, the growth behavior of the (111) face is dominated by the screw dislocation. When we refer to their experimental results, the growth behavior on the {0001} face of ice crystals growing at −28.5°C may show the same tendency as that on the (111) face of Ba $(NO_3)_2$ crystals. That is, in Fig. 4, solid triangles may be the growth hillocks formed by screw dislocations, while solid circles may be those formed by mixed dislocations. Here, the slope of growth hillocks on the {10$\bar{1}$0} face P_P is steeper than that on the {0001} face P_B. This tendency also holds for plate-like ice crystals grown at −15 and −7°C (Gonda *et al.* 1994; Matsuura, 1992) .

Figure 5 shows a possible explanation of the formation mechanism of a plate-like ice crystal grown at −28.5°C and low supersaturation. When the slope of a growth hillock formed on the {10$\bar{1}$0} face P_P is steeper than that on the {0001} face P_B , the normal growth rate of the {10$\bar{1}$0} face R_P becomes larger than that of the {0001} face R_B because the normal growth rate is proportional to the slope of the growth hillock. Where P_P= tan θ_P, P_B= tan θ_B. As a result, a plate-like ice crystal grows. In other words, when
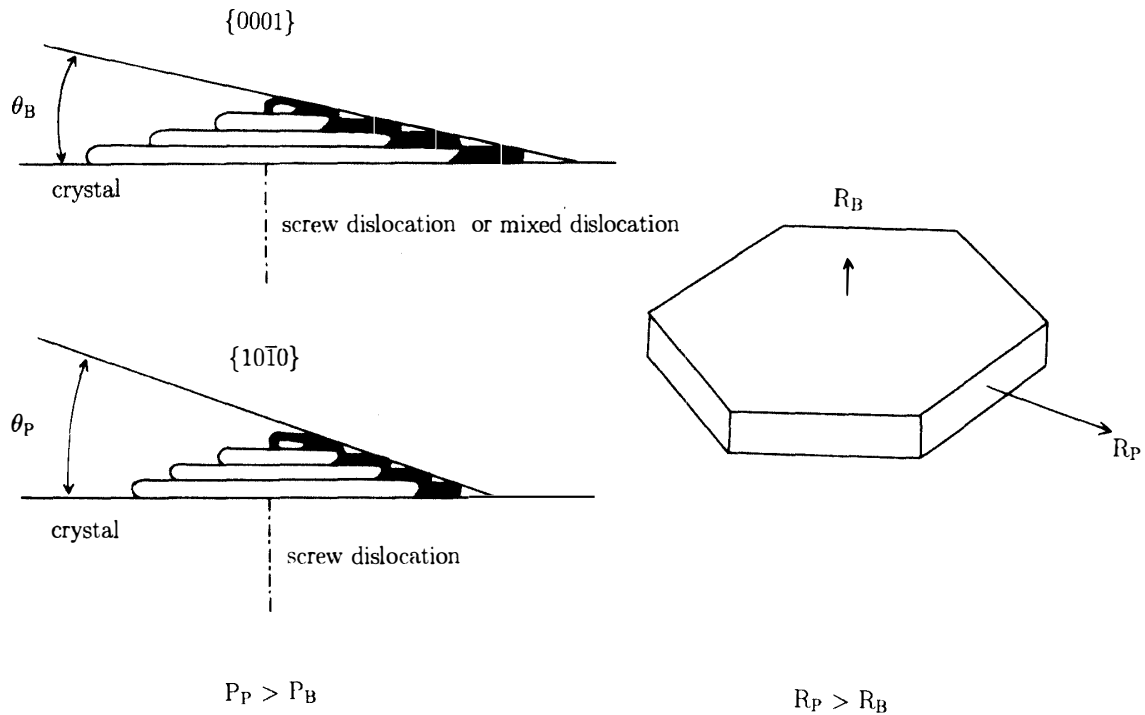
Fig. 5. Schematic diagram of the formation mechanism of a plate-like ice crystal grown at low temperature and low supersaturation.

both the $\{10\bar{1}0\}$ and $\{0001\}$ faces of a plate-like ice crystal grow by the BCF mechanism, the specific free energy of a step at the vapor/ice interface (step energy) γ of the $\{10\bar{1}0\}$ and $\{0001\}$ faces is $\gamma_{\{10\bar{1}0\}}=3.23\times10^{-14}$ erg/molecule and $\gamma_{\{0001\}}=6.40\times10^{-14}$ erg/molecule, respectively. Accordingly, when the relationship $\gamma_{\{10\bar{1}0\}}<\gamma_{\{0001\}}$ is applicable, a plate-like ice crystal grows.

In addition, from the present experimental results, thin plate-like ice crystals observed at South Pole Station can be interpreted by considering the combination of open circles (P_P) and solid circles (P_B) in Fig. 4.

5. Conclusions

The supersaturation dependences on the slope of growth hillocks on the $\{10\bar{1}0\}$ face P_P and on the $\{0001\}$ face P_B were measured to study the formation mechanism of plate-like ice crystals grown at $-28.5°C$ and low supersaturation. The result is that both the $\{10\bar{1}0\}$ and $\{0001\}$ faces of ice crystals grown at this condition grow by the Burton-Cabrera-Frank (BCF) mechanism and when the relationship $P_P>P_B$ holds, plate-like ice crystals grow.

References

BURTON, W.K., CABRERA, N. and FRANK, F.C. (1951): The growth of crystals and the equilibrium structure of their surfaces. Philos. Trans. R. Soc. London, A243, 299–358.

GONDA, T. (1983): Morphology of ice crystals growing in free fall at the temperature between –40 and

−140°C. Mem. Natl Inst. Polar Res., Spec. Issue, **29**, 110–120.

GONDA, T. and KOIKE, T. (1982): Growth rates and growth forms of ice crystals grown from the vapor phase. J. Cryst. Growth, **56**, 259–264.

GONDA, T., SEI, T. and WADA, M. (1986): Growth form of ice crystals grown in air at low supersaturation and their growth mechanism. Mem. Natl Inst. Polar Res., Spec. Issue, **45**, 30–37.

GONDA, T., MATSUURA, Y. and SEI, T. (1994): *In situ* observation of vapor-grown ice crystals by laser two-beam interferometry. J. Cryst. Growth, **142**, 171–176.

KIKUCHI, K. and HOGAN, A.W. (1979): Properties of diamond dust type ice crystals observed in summer season at Amundsen-Scott South Pole Station, Antarctica. J. Meteorol. Soc. Jpn., **57**, 180–190.

KOBAYASHI, T. (1961): The growth of snow crystals at low supersaturation. Philos. Mag., **6**, 1363–1370.

KURODA, T. and LACMANN, R. (1982): Growth kinetics of ice from the vapour phase and its growth forms. J. Cryst. Growth, **56**, 189–205.

MAIWA, K., TSUKAMOTO, K. and SUNAGAWA, I. (1990): Activities of spiral growth hillocks on the (111) faces of Barium Nitrate crystals growing in an aqueous solution. J. Cryst. Growth, **102**, 43–53.

MATSUURA, Y. (1992): The study of the growth mechanism of ice crystals and ice crystal habit by two-beam interferometry. Master Dissertation, Science Univ. of Tokyo (in Japanese).

NAKAYA, U. (1954): Snow Crystals, Natural and Artificial. Harvard Univ. Press, 248–252.

VERMA, A.R. (1953): Crystal Growth and Dislocations. London, Butterworths, 116–146.